Sensors and Materials, Vol. 37, No. 1 (2025) 381–390
MYU Tokyo

S & M 3915

Microstructure and Optical and Piezoelectric Properties of Polyvinylidene Fluoride/ZnO Nanowires for Tactile Sensors

Ming-Cheng Kao,[1*] Jun-Hong Weng,[2] Chih-Hung Chiang,[3]
Kai-Huang Chen,[4] and Tsung-Kuei Kang[5]

[1]Graduate Institute of Aeronautics, Department of Information and Communication Engineering, Chaoyang University of Technology, Taichung 413310, Taiwan
[2]Graduate Institute of Aeronautics, Chaoyang University of Technology, Taichung 413310, Taiwan
[3]Department of Electrical Engineering, Tunghai University, Taichung 407224, Taiwan
[4]Department of Electronic Engineering, Cheng Shiu University, Kaohsiung 83347, Taiwan
[5]Department of Electronic Engineering, Feng Chia University, Taichung 407102, Taiwan

(Received August 5, 2024; accepted December 26, 2024)

Keywords: ZnO, PVDF, pressure sensor, piezoelectric

Polyvinylidene fluoride (PVDF)/ZnO nanowire arrays were prepared on polydimethylsiloxane (PDMS) substrates for piezoelectric pressure sensor applications by the chemical bath deposition method. The effects of three different catalysts, namely, NaOH, NH_4OH, and $C_6H_{12}N_4$ (HMT), on the crystal structure, surface structure, and optical characteristics of ZnO nanowires have been studied. The piezoelectric sensing properties of pressure sensors formed by coating PVDF on ZnO nanowires were also studied under different forces. The results showed that the ZnO nanowires obtained with HMT have a hexagonal wurtzite crystal structure with a good *c*-axis (002) preferred orientation, as well as the largest length of 5800 nm and a length-to-width ratio of 72.5. The maximum sensitivity of the sensor with the ZnO nanowire length of 5800 nm is 61.1 mV/N. In addition, the sensor exhibits an optimized linear response within the applied pressure range of 0.1–1.2 N.

1. Introduction

Pressure sensors are sensors that detect and measure physical touch or pressure. These sensors are used in various applications, including robotics, consumer electronics, medical devices, and industrial automation.[1–4] In recent years, many researchers have studied the applications of materials such as ZnO, $Pb(ZrTi)O_3$ (PZT), and polyvinylidene fluoride (PVDF) in pressure sensors. Because of their superior piezoelectric properties and high sensitivity, these materials are suitable for pressure sensing applications.[5–8] Among these materials, ZnO is a piezoelectric ceramic that creates electrical signals in reaction to applied mechanical stress, making it ideal for converting mechanical pressure into electrical signals. PZT exhibits a high sensitivity and piezoelectric property, making it suitable for detecting subtle changes in pressure. PVDF is ideal for wearable pressure sensors because of its excellent flexibility and scalability in

*Corresponding author: e-mail: kmc@cyut.edu.tw
https://doi.org/10.18494/SAM5277

ISSN 0914-4935
https://myukk.org/

large-area production. The composite of ZnO nanowires and PVDF films offers multiple advantages for pressure sensing applications owing to their unique properties, including high length-to-width ratio, large surface area, excellent mechanical properties, high responsiveness, and piezoelectric properties. For example, Deng *et al.* used electrospinning technology to prepare cowpea-structured PVDF/ZnO nanofiber sensors that showed a sensitivity of 0.403 mV/N in bending and pressing modes.[9] Taleb *et al.* prepared a ZnO/PVDF-TrFE(Trifluor oethylene) piezoelectric composite flexible piezoelectric composite film as a pressure sensor through spraying and casting methods with a sensitivity of 18.5 mV/N.[10] Chen *et al.* used an electrospinning method to prepare a P(VDF-TrFE)/ZnO nanofiber pressure sensor with a sensitivity of 8.30 mV/kPa.[11]

However, there are few research studies on the chemical bath deposition method to prepare the PVDF/ZnO nanowire pressure sensors. The chemical bath deposition method has the advantages of low temperature, energy saving, controllable morphology, high purity, and good crystallinity. In this study, ZnO nanowires with high length-to-width ratio and large surface area were deposited by the chemical bath deposition method, allowing flexibility in sensor design and fabrication. These nanowires can be integrated into flexible substrates, enabling the development of bendable and stretchable pressure sensors. This helps improve the durability and reliability of pressure sensors in harsh operating environments and adapts to irregular surfaces. In this investigation, the ZnO nanowires were coated with a piezoelectric polymer film of PVDF, which can effectively add an additional layer of piezoelectric material. PVDF is a piezoelectric material, which means that it generates an electric charge under mechanical stress or applied pressure. By coating ZnO nanowires with a PVDF film, the pressure stimulation for the sensitivity of the sensor can be improved. When pressure is applied to the sensor, both the ZnO nanowires and the PVDF film deform, producing a measurable electrical signal to detect and quantify the applied pressure. The integration of ZnO nanowires and PVDF films improves the overall responsiveness and efficiency of the pressure sensor. In this study, PVDF/ZnO nanowires were prepared on a polydimethylsiloxane (PDMS) substrate coated with silver electrodes. The effects of catalysts (NaOH, NH_4OH, and $C_6H_{12}N_4$ (HMT)) on the structure and optical properties of ZnO nanowires are discussed in this study. We also explore the effects of catalysts on the output voltage and sensitivity of composite pressure sensors.

2. Materials and Methods

Before synthesizing ZnO nanowires, a ZnO thin film was employed as a seed layer to facilitate their growth. Zinc acetate and propylene glycol were utilized to prepare the ZnO precursor, with a ZnO concentration of 0.5 M. The solution was continuously mixed in a 60 ℃ water bath for three hours to achieve a clear and uniform mixture. Spin coating at 3000 rpm for 30 s was carried out to deposit the seed layer onto the PDMS substrate. The specimens were heat-treated at 600 ℃ for two minutes to establish a ZnO seed layer on the substrate. ZnO nanowires were synthesized using a hydrothermal technique. The zinc acetate $[Zn(C_2H_3O_2)_2{\cdot}2H_2O]$ solution of 10 mM was mixed with three different catalysts of 0.15 mol NaOH, 0.15 mol NH_4OH, and 0.2 mol HMT at 90 ℃ for 6 h to obtain the ZnO nanowire. To

remove the solvent, the samples were cleaned with deionized water and allowed to dry naturally at ambient temperature. The PVDF films were deposited on ZnO nanowires using a solution process coating technology. The piezoelectric polymer materials should be doped in dimethylformamide (DMF) organic solvent, followed by thorough stirring to ensure complete dissolution. The PVDF precursor solution was distributed onto the substrate surface by spin coating. After coating, the PVDF/ZnO nanowires were heated in a heating furnace at 120 ℃ for one hour to eliminate DMF and solidify the PVDF layer. This step promotes solvent evaporation and crystallization of the PVDF polymer, helping to enhance the structural integrity and piezoelectric properties of the PVDF film. A conductive copper foil was attached to both sides of the PVDF film to form the electrodes of the pressure sensor. Finally, the PDMS layer was grown on the PVDF film by spin coating to complete the structure of the pressure sensor shown in Fig. 1.

The crystalline characteristics of ZnO nanowires were evaluated using an X-ray diffractometer (XRD) with Cu Kα radiation (λ = 1.5418 Å). Field emission scanning electron microscopy (FE-SEM) was used to characterize the sample surface morphologies. Photoluminescence (PL) spectroscopy, employing a He-Cd laser at 325 nm, was conducted to measure the optical emissions of the ZnO nanowires across the 325–600 nm wavelength range. The Raman spectra of the samples were measured with an excitation wavelength of 532 nm from an argon laser to investigate the structural properties and vibrational modes of the ZnO nanowires. To evaluate the piezoelectric response of the ZnO-nanowire-based pressure sensor, a charge amplifier was used to convert the charge signal generated by the piezoelectric PVDF/ZnO nanowire pressure sensor into an output voltage. When the PVDF/ZnO nanowire pressure sensor is pressed with a finger, a digital force gauge records the pressing force. A digital oscilloscope was used to acquire and postprocess the output voltage of the pressure sensor.

3. Results and Discussion

The crystallinity of ZnO nanowires was investigated using X-ray diffraction. The XRD crystallinities of ZnO nanowires prepared using different catalysts (NaOH, NH_4OH, and HMT) are shown in Fig. 2. All XRD patterns can be classified as the structure of hexagonal wurtzite ZnO (JCPDS card number 36-1451). The strongest peak of ZnO in terms of crystal orientation corresponds to the (002) plane, showing a strong preferred orientation in the [001] direction. The results revealed that the (002) diffraction peak intensity of the ZnO nanowires prepared using

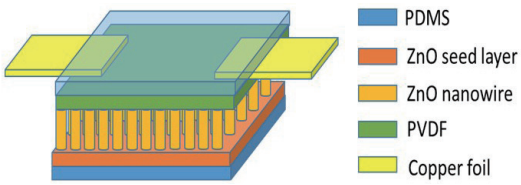

Fig. 1. (Color online) Structure of robotic pressure sensor.

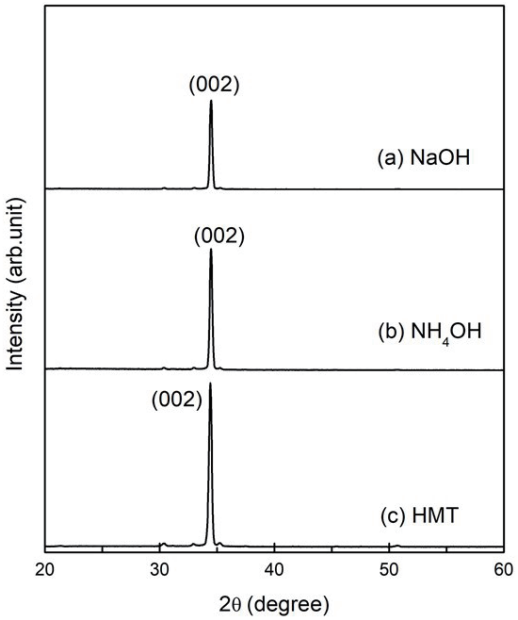

Fig. 2. XRD analysis results of ZnO nanowires prepared with (a) NaOH, (b) NH_4OH, and (c) HMT catalysts.

the HMT catalyst is the highest, showing excellent crystallinity compared with other samples. The study revealed that catalysts considerably affect the crystallinity and structural properties of ZnO nanowires. Among the catalysts studied, HMT promotes superior nucleation and growth for ZnO crystallization compared with NaOH and NH_4OH.

The plane and cross-sectional SEM images of ZnO nanowires prepared with NaOH, NH_4OH, and HMT catalysts are shown in Fig. 3. The results showed that the morphology of the ZnO nanowires was affected by different catalysts. The average diameter, length, and length-to-width ratio of the ZnO nanowires, derived from the analysis of Fig. 3, are summarized in Table 1. The ZnO nanowires synthesized using NaOH, NH_4OH, and HMT catalysts exhibit average diameters of 40, 60, and 80 nm and corresponding lengths of 1250, 3800, and 5500 nm, respectively. According to the observed results, the diameter, length, and length-to-width ratio of the the ZnO nanowires prepared with the HMT catalyst are the largest. The reason could be that HMT decomposes amines in aqueous solution, providing OH– groups for ZnO nucleation on the surface of the substrate. With the slow amine cleavage rate of HMT, the pH value of the water remains relatively stable, leading to a decreased mole concentration of the complexes of metal ions.[12] The precipitation response of ZnO can be determined at a low degree of supersaturation to facilitate heterogeneous growth, making it easy for ZnO nanowire crystals to grow in columnar shapes.[13] The addition of NaOH and NH_4OH catalysts to the aqueous solution considerably elevates the pH, resulting in an increased concentration of metal complexes. ZnO predominantly undergoes uniform nucleation, leading to nanowires with reduced diameter and smaller length.[14]

Figure 4 shows the Raman spectra for the ZnO nanowires to investigate the effect of different catalysts on the microstructural and vibrational properties of the nanowires. The Raman active-zone-center optical phonons at Γ point of the Brillouin zone can be denoted by the following

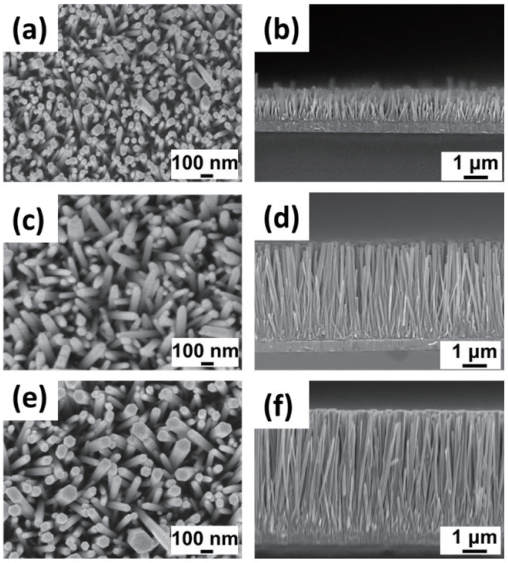

Fig. 3. Plane and cross-sectional SEM images of ZnO nanowires synthesized using (a) and (b) NaOH, (c) and (d) NH_4OH, and (e) and (f) HMT catalysts.

Table 1
Structural properties of ZnO nanowires grown using various catalysts.

Reaction catalysts	Nanowire length (nm)	Nanowire diameter (nm)	Nanowire length-to-width ratio
NaOH	1250	40	31.3
NH_4OH	3800	60	63.3
HMT	5800	80	72.5

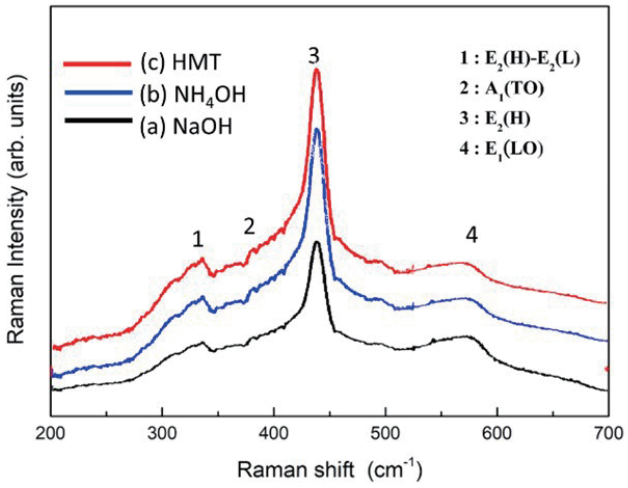

Fig. 4. (Color online) Raman spectra for ZnO nanowires synthesized using (a) NaOH, (b) NH_4OH, and (c) HMT catalysts.

representations: $\Gamma_{opt} = A_1 + E_1 + 2E_2 + 2B_1$. The B_1 modes are silent modes, the A_1 and E_1 modes are polar and split into transverse optical (TO) and longitudinal optical (LO) phonons, whereas the E_2 modes are nonpolar and Raman active only.[15] The Raman scattering peaks located at 331, 383, 436, and 573 cm^{-1} can be observed for all nanowires, as shown in Fig. 4. The peak at 331 cm^{-1} occurs under the resonance condition and can be interpreted as the second-order Raman spectra arising from zone boundary phonons $E_2(H)$–$E_2(L)$. The peaks located at 383 cm^{-1} are assigned to A_1 symmetry with the TO mode. The $E_2(H)$ mode centered at 436 cm^{-1} indicates the crystallization of the nanowires for the wurtzite hexagonal ZnO involving oxygen atoms.[16] The E2(H) mode Raman peak intensity of ZnO nanowires using HMT is higher than when using NaOH and NH_4OH, which indicates that ZnO nanowires using HMT have higher crystallinity, which is consistent with XRD analysis. The bands at 573 cm^{-1} correspond to E_1 symmetries with LO modes. It is generally accepted that the $E_1(LO)$ is related to the formation of defects in ZnO. Therefore, the progressive appearance and higher intensity of the E1(LO) Raman peak in ZnO nanowires synthesized using NaOH and NH_4OH suggest a higher concentration of defects, such as oxygen vacancies and zinc interstitials, in these nanowires compared with those synthesized using HMT.[17]

The room-temperature PL spectra of ZnO nanowires were determined in different aqueous solutions of zinc acetate and zinc nitrate at an excitation wavelength of 325 nm and are shown in Fig. 5. The PL spectrum of ZnO nanowires at room temperature shows two main peaks: one is that of ultraviolet emission near 374 nm, and the other is that of yellow emission from 470 to 650 nm. Ultraviolet emission is mainly produced by exciton emission near the band edge. This is caused by the recombination of free excitons as a results of the collision of excitons with each other.[18] The yellow light emission can be called deep-energy-level emission, which is caused by the recombination of electron holes and oxygen vacancies generated by illumination.[19–21] The research results showed that the intensity of the ultraviolet emission of nanowires synthesized using HMT is stronger than those of ZnO nanowires synthesized using NaOH and NH_4OH, indicating that the nanowires synthesized using HMT have better crystallinity. In addition,

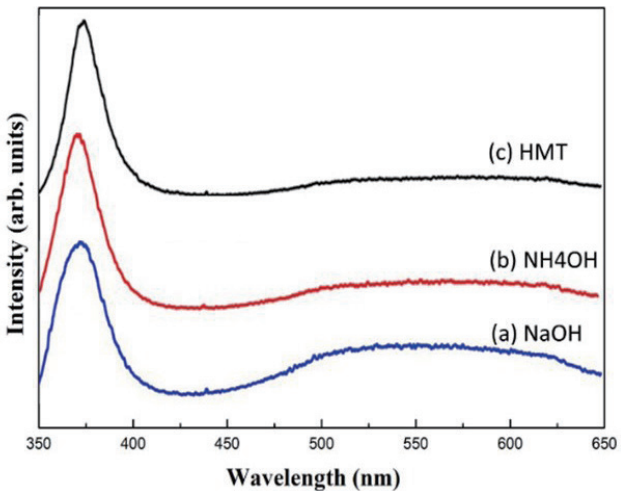

Fig. 5. (Color online) Spectra of ZnO nanowires synthesized using (a) NaOH, (b) NH_4OH, and (c) HMT catalysts.

compared with nanowires synthesized using HMT, ZnO nanowires synthesized using NaOH and NH_4OH have strong and broad yellow-green emission centered at ~560 nm. This indicates that the ZnO nanowires synthesized using NaOH and NH_4OH have defects such as surface oxygen vacancies and structural defects. The origin of the yellow peak can be attributed to point defects such as Zn, while the green-band emission is believed to be the superposition of different PL bands including V_{Zn}- and V_O-related bands. The PL results are consistent with those of Raman studies.

The piezoelectric response of the nanowire pressure sensor is measured using a charge amplifier, which transforms the sensor's charge signal into an output voltage that is recorded and analyzed using a digital oscilloscope. Figure 6 shows the voltage response of the PVDF/ZnO nanowire pressure sensor with different catalysts. The ZnO nanowire pressure sensors under a force of 1 N demonstrated voltage peaks of 10, 35, and 53 mV when NaOH, NH_4OH, and HMT were used as catalysts, respectively. The voltage peaks of PVDF/ZnO nanowire pressure sensors using NaOH, NH_4OH, and HMT are 22, 40, and 61 mV, respectively. Fabricating the PVDF/ZnO nanowire pressure sensor with HMT leads to a high voltage peak amplitude owing to its maximum length-to-width ratio, which enhances radial stress under equal pressure, thereby increasing the piezoelectric dislocation along the *c*-axis.[22] Furthermore, the output voltage of the pressure sensors was enhanced when the polymer material was applied to the ZnO

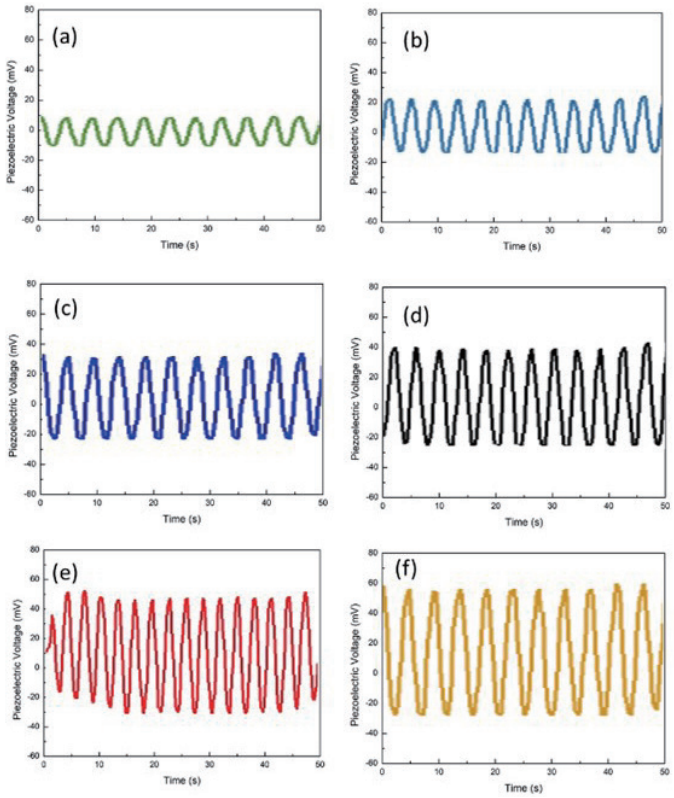

Fig. 6. (Color online) Analysis of piezoelectric sensing voltage differences in pressure sensors with ZnO nanowires synthesized using (a) and (b) NaOH, (c) and (d) NH_4OH, and (e) and (f) HMT catalysts. (a), (c), and (d) are the pure ZnO nanowires, and (b), (d), and (f) are the PVDF/ZnO nanowires.

nanowires. This can be attributed to the piezoelectric nature of PVDF, which generates charges under mechanical stress or pressure, thereby enhancing the detection of the pressure sensor. The integration of ZnO with PVDF films improves the overall responsiveness of the sensor and performance under applied pressure.[23]

The piezoelectric response of the pressure sensor was evaluated under different applied forces to analyze its dependence on external pressure. The associated voltage peak amplitude was derived from the dynamic piezoelectric response waveforms of the pressure sensors. In Fig. 7, the voltage response of the sensor is shown under different applied forces. The results demonstrate a linear increase in voltage response corresponding to the applied force. Table 2 presents the sensitivities of ZnO nanowire pressure sensors fabricated using different catalysts. The ZnO nanowire pressure sensors using NaOH, NH_4OH, and HMT catalysts exhibit sensitivities of 8.8, 20.6, and 50.1 mV/N, respectively. The sensitivities of PVDF/ZnO nanowire pressure sensors using NaOH, NH_4OH, and HMT are 31.8, 39.6, and 61.1 mV/N, respectively. The PVDF/ZnO nanowire pressure sensor fabricated with HMT exhibits a high sensitivity of up to 61.1 mV/N, attributable to the significant length-to-width ratio along the *c*-axis orientation and the incorporation of PVDF.

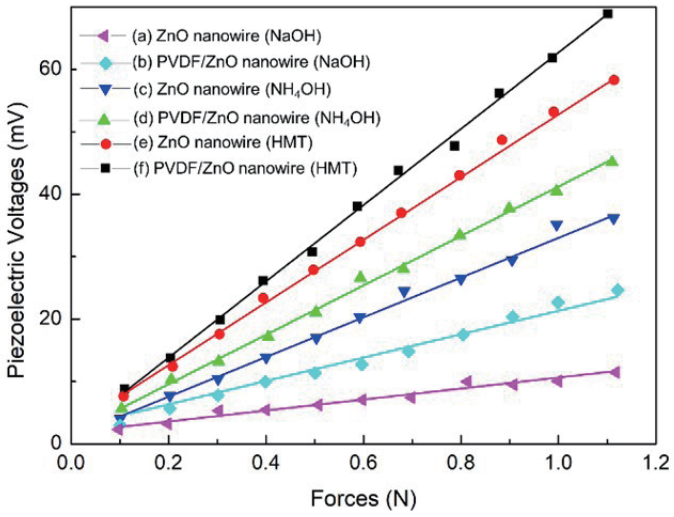

Fig. 7. (Color online) Piezoelectric output voltages of pressure sensors subjected to various pressure conditions.

Table 2
Analysis of output voltage and detection differences among pressure sensors.

Pressure sensors	Reaction catalysts	Piezoelectric detection voltages (mV)	Sensitivity (mV/N)
ZnO nanowire	NaOH	10	8.8
	NH_4OH	35	20.6
	HMT	53	50.1
PVDF/ZnO nanowire	NaOH	22	31.8
	H_4OH	40	39.6
	HMT	61	61.1

4. Conclusions

In this study, PVDF/ZnO nanowire piezoelectric pressure sensors were fabricated on PDMS substrates by chemical bath deposition methods. Catalysts (NaOH, NH4OH, and HMT) were studied for their effects on the lattice structure, surface features, optical properties, and piezoelectric characteristics of ZnO nanowires. The results showed that the diameter, length, and length-to-width ratio of the ZnO nanowires prepared using the HMT catalyst are the largest. The PVDF/ZnO nanowire pressure sensor fabricated with HMT exhibits the highest voltage peak amplitude and a sensitivity of up to 61.1 mV/N, attributed to the large length-to-width ratio along the *c*-axis orientation and the incorporation of PVDF. This piezoelectric pressure sensor shows promise for applications in robotic electronic skin for pressure sensing.

Acknowledgments

This work was sponsored by the National Science Council of the Republic of China under Grant No. NSTC 113-2637-E-324-001.

References

1 V. S. Kumar and C. Krishnamoorthi: Sens. Actuators, A **321** (2021) 112582. https://doi.org/10.1016/j.sna.2021.112582
2 Z. J. Tang, Z. Wang, J. Q. Lu, and N. G. Q. Ma: Int. J. Adv. Rob. Syst. **16** (2019) 1. https://doi.org/10.1177/17298814198798
3 N. F. Lepora, A. Church, C. de Kerckhove, R. Hadsell, and J. Lloyd: IEEE Rob. Autom. Lett. **4** (2019) 2101. https://doi.org/10.1109/LRA.2019.2899192
4 C. X. Wu, T. W. Kim, J. H. Park, B. Koo, S. Y. Sung, J. J. Shao, C. Zhang, and Z. L. Wang: ACS Nano **14** (2020) 1390. https://doi.org/10.1021/acsnano.9b07165
5 Y. S. Tan, K. Yang, B. Wang, H. Li, L. Wang, and C. X. Wang: Nano Res. **14** (2021) 3969. https://doi.org/10.1007/s12274-021-3322-2
6 T. Siponkoski, M. Nelo, J. Palosaari, J. Peräntie, M. Sobocinski, J. Juuti, and H. Jantunen: Compos. B Eng. **80** (2015) 217. https://doi.org/10.1016/j.compositesb.2015.05.018
7 T. Yang, H. Pan, G. Tian, B. Zhang, D. Xiong, Y. Gao, C. Yan, X. Chu, N. Chen, S. Zhong, L. Zhang, W. Deng, and W. Yang: Nano Energy **72** (2020) 104706. https://doi.org/10.1016/j.nanoen.2020.104706
8 J. Yang, Q. S. Chen, F. Xu, H. X. Jiang, W. L. Liu, X. Q. Zhang, Z. X. Jiang, and G. D. Zhu: Adv. Electron. Mater. **6** (2020) 1. https://doi.org/10.1002/aelm.202000578
9 W. Deng, T. Yang, L. Jin, C. Yan, H. Huang, X. Chu, Z. Wang, D. Xiong, G. Tian, Y. Gao, H. Zhang, and W. Yang: Nano Energy **55** (2019) 516. https://doi.org/10.1039/d4ma00283k
10 S. Taleb, W. M. van Lingen, and M. Acuautla: Mater. Adv. **5** (2024) 7671. https://doi.org/10.1039/d4ma00283k
11 Y. Chen, C. Qin, Q. Sun, and M. Wang: Sens. Actuators, A **379** (2024) 115970. https://doi.org/10.1016/j.sna.2024.115970
12 K. Govender, D. S. Boyle, P. B. Kenway, and P. O'Brien: J. Mater. Chem. **14** (2004) 2575.
13 L. E. Greene, M. Law, J. Goldberger, F. Kim, J. C. Johnson, Y. Zhang, R. J. Saykally, and P. Yang: Angew. Chem. Int. **42** (2003) 3031. https://doi.org/10.1039/B404784B
14 L. Vayssieres, K. Keis, A. Hagfeldt, and S. Lindquist: Chem. Mater. **13** (2001) 4395. https://doi.org/10.1021/cm011160s
15 B. C. Cheng, Y. H. Xiao, G. S. Wu, and L. D. Zhang: Appl. Phys. Lett. **84** (2004) 416. https://doi.org/10.1063/1.1639131
16 S. K. Sharma and G. J. Exarhos: Solid State Phenom. **55** (1997) 32. https://doi.org/10.4028/www.scientific.net/SSP.55.32
17 J. J. Wu and S. C. Liu: J. Phys. Chem. B **106** (2002) 9546. https://doi.org/10.1021/jp025969j

18 Y. W. Chen, Y. C. Liu, S. X. Lu, C. S. Xu, C. L. Shao, C. Wang, J. Y. Zhang, Y. M. Lu, D. Z. Shen, and X. W. Fan: J. Chem. Phys. **123** (2005) 134701. https://doi.org/10.1063/1.2009731
19 K. Vanheusden, C. H. Seager, W. L. Warren, D. R. Tallant, and J. A. Voigt: Appl. Phys. Lett. **68** (1996) 403. https://doi.org/10.1063/1.116699
20 X. L. Wu, G. G. Siu, C. L. Fu, and H. C. Ong: Appl. Phys. Lett. **78** (2001) 2285. https://doi.org/10.1063/1.1361288
21 S. Rajamanickam, S. M. Mohammad, and Z. Hassan: Colloids Interface Sci. Commun. **38** (2020) 100312. https://doi.org/10.1016/j.colcom.2020.100312
22 W. Deng, L. Jin, B. Zhang, Y. Chen, L. Mao, H. Zhang, and W. Yang: Nanoscale **8** (2016) 16302. https://doi.org/10.1039/C6NR04057H
23 A. Fraleoni-Morgera, I. Cesini, P. Kumar, and C. M. Oddo: ChemNanoMat **6** (2020) 15. https://doi.org/10.1002/cnma.201900620